

Article

Efficient Image Registration for Underwater Optical Mapping Using Geometric Invariants

Armagan Elibol *  and Nak Young Chong 

School of Information Science, Japan Advanced Institute of Science and Technology, Ishikawa 923-1292, Japan; nakyoung@jaist.ac.jp

* Correspondence: aelibol@jaist.ac.jp; Tel.: +81-0761-51-1362

Received: 25 April 2019 ; Accepted: 31 May 2019 ; Published: 5 June 2019



Abstract: Image registration is one of the most fundamental and widely used tools in optical mapping applications. It is mostly achieved by extracting and matching salient points (features) described by vectors (feature descriptors) from images. While matching the descriptors, mismatches (outliers) do appear. Probabilistic methods are then applied to remove outliers and to find the transformation (motion) between images. These methods work in an iterative manner. In this paper, an efficient way of integrating geometric invariants into feature-based image registration is presented aiming at improving the performance of image registration in terms of both computational time and accuracy. To do so, geometrical properties that are invariant to coordinate transforms are studied. This would be beneficial to all methods that use image registration as an intermediate step. Experimental results are presented using both semi-synthetically generated data and real image pairs from underwater environments.

Keywords: image registration; image mosaicking; optical mapping; geometric invariants

1. Introduction

Owing to the recent developments of robotic platforms carrying cameras, it is possible to obtain optical data from places where a human cannot access (e.g., Mars, aerial imaging, seabed, and many others.). Processing the optical data to have a 2D-map (or mosaic) of the visited area has been very important for different science communities (e.g., remote sensing, geology, ecology, marine science, environmental science and several others) and there has been a high demand for creating maps from gathered images using image mosaicking methods. Image mosaicking can be defined as creating a big image by composing relatively smaller images. Image mosaicking requires a good harmony of different steps. One of the most crucial steps in image mosaicking (especially when there is no additional sensor information except vision) is to find the transformation (motion) between overlapping image pairs and this process is referred to as image registration [1]. Lately, image registration is done through finding and matching some salient points (called as features) in images. Four main steps for feature-based image registration are (1) feature extraction, (2) computing feature descriptors, (3) descriptor matching and (4) computing a transformation between image coordinate frames using robust estimation methods. During the descriptor matching step, there usually occur some matched pairs that do not follow the transformation (or equivalently the relative motion of the robotic platform) between images and they are called outliers. These outliers are rejected using probabilistic methods based on robust estimation (mainly using a Random Sampling Consensus (RANSAC) algorithm [2]). Afterward, the transformation between images is calculated by minimizing a pre-defined cost function on feature point positions [3]. The success of this minimization depends on whether the matching between the features of the two images is free of outliers or not. The existence and the number of these outliers have a direct effect on the performance of the minimization used. Particularly in large scale differences

between images, the number of mismatches is often high (e.g., Figure 1). This causes an incorrect estimation of the coordinate transformation between the two images. Moreover, the probabilistic nature of RANSAC-based methods could bring a computational burden as they work in an iterative manner. Our main objective is to develop a method to remove the limitations of the robust estimation methods used in feature-based image registration especially for the cases where outliers are more numerous than the inliers and also to improve the performance of robust estimation methods in terms of computational cost and accuracy. This would greatly improve most of the existing methods that make use of feature-based image registration as an intermediate step as well as making it possible to match image pairs with a large scale difference. This would be very useful for mapping, 3D reconstruction, object detection, localization applications and many others using robotics platforms.

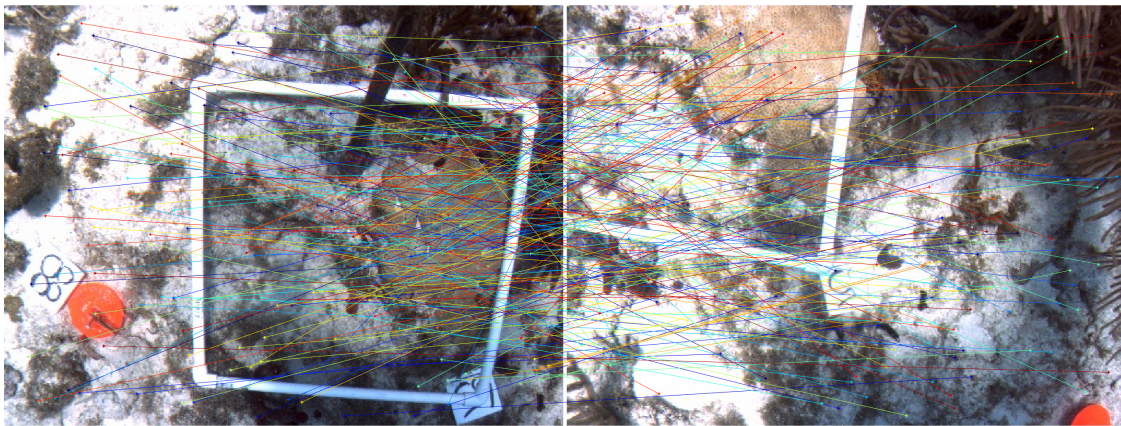


Figure 1. Example of extracted and matched features between images with a relatively large scale difference. RANSAC would be applied to remove outliers; however, it is likely to fail to work accurately due to the high presence of outliers.

There have been several methods proposed to improve RANSAC. MSAC (M-Estimator Sample Consensus) [4] is based on RANSAC. The outcome may significantly change according to the error threshold (to decide whether the data obey the estimated model or not. In other words, to decide inlier or outlier) selected in RANSAC. In MSAC, there is also a threshold check for inliers in addition to outliers like in RANSAC. Therefore, MSAC is a slightly improved version of RANSAC. The difference between MLESAC (Maximum Likelihood Estimation Sample) [4] and RANSAC is in the step of checking whether the estimated model suits the data or not. Instead of counting the inliers, MLESAC uses Maximum-Likelihood estimation to decide. Tordoff and Murray (Guided-MLESAC [5]) showed that, in the case of some probabilistic information known a priori about the dataset, how this can be used in the MLESAC algorithm and the required number of iterations can be reduced. PROSAC (Progressive Sample Consensus) [6] proposed an enhanced sampling algorithm instead of doing it randomly as in RANSAC. The features were ranked according to similarity scores of their descriptors and samples selected through their ranking. Raguram et al. [7] presented a comparison of RANSAC based methods and also adaptively changing/calculating the total number of needed iterations by computing the outlier ratio. This allowed for running RANSAC faster. Senthilnath et al. [8] proposed a method to register images coming from different sensors by using a genetic algorithm. They used more criteria to find the transformation between images. Similarly, Le et al. [9], proposed an efficient sampling technique using shape prior information for fitting a cylindrical object from a 3D point cloud using RANSAC. Both studies in [8] and [9] provide a base for our work in this paper. The main disadvantages of all these aforementioned methods are iterative and probabilistic. Although they perform well in the cases where the outlier ratio is low, they require a lot of iterations in the cases where outlier ratio is getting higher. Marszalek and Rokita [10] proposed a method for establishing correspondences between astronomical images using a single invariant property of distance ratio.

In this paper, we extend their work by integrating the usage of different invariants and introducing a confidence level measure to decide whether robust estimation can be discarded or not.

In this paper, our objective is to discuss the possible usage of geometrical invariants in order to enhance the feature-based image registration framework in unmanned scene mapping and reduce the iterations needed in probabilistic methods in the framework. The next section provides an overview of the planar transformations used in this study while Section 3 details on integrating the geometrical invariants into a feature-based image registration framework. Section 4 presents experimental results and Section 5 summarizes some conclusions.

2. Overview of Used Planar Transformations

In this study, we focus on 4-Degree-of-Freedom (DOF) similarity and the 6-DOF affine motion model represented by 2D planar transformations as they provide good enough DOFs for a robot motion moving in a relatively controlled environment with a downlooking camera whose optical axis is approximately kept perpendicular to the seabed.

Similarity Transformations A Similarity transformation is a scale included version of Euclidean transformation. The rotation is around an optical axis and scale in our context refers to the altitude changes of an underwater robot. A similarity transformation can be decomposed as follows [3]:

$$\mathbf{H}_s = \begin{bmatrix} \mathbf{SR} & \mathbf{t} \\ \mathbf{0}^T & 1 \end{bmatrix}_{3 \times 3}, \quad \mathbf{SR} = \underbrace{\begin{bmatrix} s & 0 \\ 0 & s \end{bmatrix}}_{\text{Scaling}} \underbrace{\begin{bmatrix} \cos \theta & -\sin \theta \\ \sin \theta & \cos \theta \end{bmatrix}}_{\text{Rotation}}, \tag{1}$$

$$sr_{11} = s \cos \theta, \quad sr_{12} = -s \sin \theta,$$

$$sr_{21} = s \sin \theta, \quad sr_{22} = s \cos \theta,$$

where θ is for rotation, s is uniform scaling on both the x - and y -axes while $\mathbf{t} = (t_x, t_y)$ is a translation vector making four DOFs in total.

Affine Transformations An affine transformation has six DOFs and it can be decomposed as follows [3]:

$$\mathbf{H}_A = \begin{bmatrix} \mathbf{A} & \mathbf{t} \\ \mathbf{0}^T & 1 \end{bmatrix}_{3 \times 3}, \tag{2}$$

where $\mathbf{A} 2 \times 2$ is the rotations and non-isotropic scalings while \mathbf{t} is the translation on the x - and y -axes. Further decomposition of \mathbf{A} can be done as follows:

$$\mathbf{A} = \begin{bmatrix} a_{11} & a_{12} \\ a_{21} & a_{22} \end{bmatrix}$$

$$= \underbrace{\mathbf{R}(\theta)}_{\text{Rotation}} \underbrace{\mathbf{R}(-\phi) \begin{bmatrix} \lambda_1 & 0 \\ 0 & \lambda_2 \end{bmatrix} \mathbf{R}(\phi)}_{\text{Deformation}}, \tag{3}$$

$$a_{11} = \frac{\cos(2\phi - \theta)}{2}(\lambda_1 - \lambda_2) + \frac{\cos \theta}{2}(\lambda_1 + \lambda_2),$$

$$a_{12} = \frac{\sin(2\phi - \theta)}{2}(\lambda_2 - \lambda_1) - \frac{\sin \theta}{2}(\lambda_1 + \lambda_2),$$

$$a_{21} = \frac{\sin(2\phi - \theta)}{2}(\lambda_2 - \lambda_1) + \frac{\sin \theta}{2}(\lambda_1 + \lambda_2),$$

$$a_{22} = \frac{\cos(2\phi - \theta)}{2}(\lambda_2 - \lambda_1) + \frac{\cos \theta}{2}(\lambda_1 + \lambda_2).$$

Visual illustration of *Rotation* and *Deformation* can be seen in Figure 2.

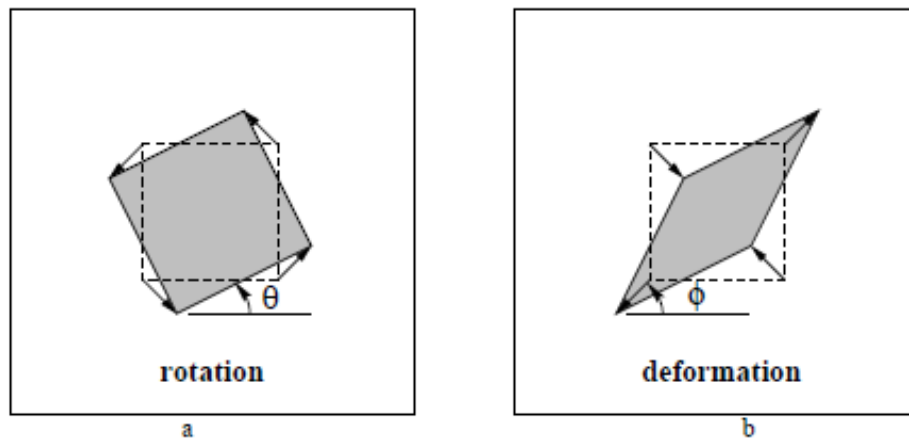


Figure 2. (a) rotation by θ ; (b) deformation by orthogonal scaling and ϕ .

3. Geometrical Invariant Extraction from Overlapping Images

The number of geometrical invariants, their properties and some hints on obtaining them from images are discussed in [3,10–12]. In this paper, we focus on obtaining geometric invariants from extracted features and putative correspondences initialized by descriptor matching. The obtained geometric invariants are used to filter correspondences before applying robust estimation. The integrated pipeline of feature-based image registration is illustrated in Figure 3. We use the geometric invariants; the ratio of lengths, angle, the ratio of areas and parallelism as they are relatively easy to obtain and their computational costs are relatively low. After matching feature descriptors, we have a list of matched point positions as ${}^A p_i = ({}^A x_i, {}^A y_i, 1)$ in image A and ${}^B p_i = ({}^B x_i, {}^B y_i, 1)$ in image B where $i = 1, 2, 3, \dots, n$ and n is the total number of correspondences.

Ratio of Lengths We compute the distance between all matched points in the same image:

$${}^A d_{i,j} = \|{}^A p_i - {}^A p_j\| \quad \text{and} \quad {}^B d_{i,j} = \|{}^B p_i - {}^B p_j\|, \quad (4)$$

where $i = 1, 2, \dots, n - 1$ and $j = i + 1, \dots, n$. Since we are interested in the ratio of lengths, we compute $r_{AB}(i, j) = \frac{{}^A d_{i,j}}{{}^B d_{i,j}}$. If the feature matching was free of outliers, the computed r values would be the same and/or very close to each other. Some extreme values are filtered out (e.g., $r < 0.1 \wedge r > 10$) assuming that the ratio does not have such extreme values. In order to find a ratio of lengths, we compute the *median* of r values. As r values may suffer truncation and/or rounding errors, we repeat the same for $r_{BA} = 1/r_{AB}$ values in order to verify. Once median of r_{AB} and r_{BA} values are found, we select all of the feature points (i, j) that provide the ratio value in a small neighborhood of selected r value (e.g., $[0.95 \times r, 1.05 \times r]$). Then, we sort the selected feature points according to their number of appearance in descending order and keep the first m of them. If the m is too small then, in the next step of the pipeline, robust estimation might fail due to not being able to find enough inliers, especially for the cases where outlier ratio is bigger than inlier ratio. If the value of m is close to the total number of correspondences (n), the total number of iteration in the robust estimation would be the same as using all correspondences and there would be no benefit of using the proposed filtering step. To decide m , we use some descriptive statistical measures (e.g., mean and standard deviation) to choose the threshold and keep the ones that appeared more than the threshold (e.g., $mean + 2 \times standarddeviation$). We also compute a confidence level as a ratio of number of entries in $[0.95 \times r, 1.05 \times r]$ and all possible r values after eliminating the extreme values.

Angle In order to use this geometric invariant, we use triangles similar to those in [10]. As descriptor matching provides putative correspondences, we use Delaunay triangulation and compute triangles in one image using correspondences. Triangles are formed by the feature positions e.g., ${}^A p_i, {}^A p_j$ and ${}^A p_k$ and similarly their correspondences in the second image, ${}^B p_i, {}^B p_j$ and ${}^B p_k$. The error between angles of corresponding triangles are computed as follows:

$$e_{ijk} = |\angle^A p_i^A p_j^A p_k - \angle^B p_i^B p_j^B p_k| + |\angle^A p_i^A p_k^A p_j - \angle^B p_i^B p_k^B p_j| + |\angle^A p_j^A p_i^A p_k - \angle^B p_j^B p_i^B p_k|, \quad (5)$$

where (i, j, k) represents the correspondences indices forming a triangle and angles can be computed using either law of cosine or difference of angles of two intersecting line segments. Indices of correspondences are selected accordingly their error value in Equation (5) smaller than a certain threshold value. We use 5° . We sort the features according to their number of appearance in triangles that are satisfying error threshold and keep the first m of them. The confidence level is similarly computed as a ratio of the total number of satisfying triangles and the total number of triangles used.

Ratio of Areas Similar to angles, we form triangles and compute the ratio of the areas of triangles. Afterward, we follow similar steps to the ratio of lengths.

Parallelism Parallel lines stay parallel after applying a transformation (except the projective model). To use this invariant, we compute the angles of all line segments of features extracted from images separately and group them with an increment of 2° in $[-\pi, \pi]$. Therefore, each group is composed of line segments that are approximately parallel. For each group, we check if they are also parallel in the second image. If they are identified as parallel, the points composing the line segments are kept in a list and at the end they are ranked according to the total number of parallel line segments in which they were involved. Similarly, we select the first m entries from the list.

Confidence Level The confidence level measure is motivated from the question “How many of the Areas/Lines out of all possibilities are following/forming the selected value of the corresponding geometric invariant?”. Let us assume that n putative correspondences are identified by the descriptor matching process and $o \in [0, 1]$ is the outlier ratio. Therefore, the total number of inliers is $n_{in} = n \times (1 - o)$. Theoretically, the ratio of the total number of triangles formed by inliers to be formed by all points assuming that points that are not collinear can be calculated using the combination formula:

$$\begin{aligned} Area_{ratio} &= \frac{\binom{n_{in}}{3}}{\binom{n}{3}} \\ &= \frac{(n_{in})(n_{in} - 1)(n_{in} - 2)}{(n)(n - 1)(n - 2)} < (1 - o)^3. \end{aligned} \quad (6)$$

Similarly, the ratio of lengths can be computed as follows:

$$Line_{ratio} = \frac{\binom{n_{in}}{2}}{\binom{n}{2}} < (1 - o)^2. \quad (7)$$

From our experiments, in the presence of a maximum of 50–60% of outliers, geometrical invariant computations are safe to continue without using robust estimators. In our experiments with real-images, we use the upper limit values computed $o = 0.6$ using for each geometric invariant. If the computed confidence level value is greater than the upper limit computed using $o = 0.6$, this means that the outlier ratio is likely to be less than the $o = 0.6$.

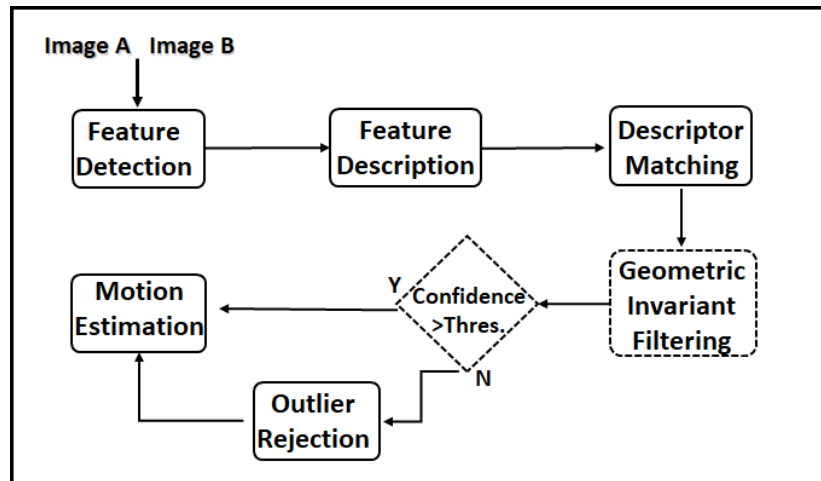


Figure 3. Geometric invariants enhanced a feature-based image registration pipeline.

4. Experimental Results

Real data from underwater images [13] and extensive simulations with synthetic data were used in order to test and validate the idea of retrieving geometrical invariant(s) from images and their usage to eliminate and/or reduce the total number of outliers. During the experiments, we assume that there is a single common motion that can be represented as a 2D planar similarity or affine transformation.

4.1. Experiment 1

In this experiment, we aim to show that geometric invariants can be obtained from correspondences when there is a high level of outliers. We detected features using Scale Invariant Feature Transform (SIFT) [14] from an image and applied a set of 20 extreme transformations [15] (details are provided in Table A1 in Appendix A) to generate their correspondences in the second image. For each transformation, we created a different number of outliers by assigning feature points randomly and tested our proposal to recover the transformation applied initially. Our test flow is presented in an algorithmic way in Algorithm 1. We provide inputs as H_i , Outlier ratios $o = [0.75, 0.80, 0.85, 0.90]$ and the number of random trials, $nbrRndTrials = 1000$. We repeat tests for a different number of total correspondences, respectively 100, 250 and 500. The results of the random trials over different outlier ratios for each transformation using three different total number of correspondences are summarized in Table 1. The first two columns are for the total number of correspondences used and the transformation while the rest of the columns represent the number of random trials in which running RANSAC *with* our proposal and *without* were able to obtain the correct value of the transformation and average number of random iterations in RANSAC for each tested outlier ratio level. The maximum number of RANSAC iteration was set to 1000 and the total number of iterations were adaptively updated during RANSAC iterations ensuring the probability of picking an outlier-free sample [16]. Since the data is noise-free, we used a small threshold (e.g., 0.5) in RANSAC to decide whether a correspondence is an outlier or not. This ensures that the outcome of the process is precisely the same as the initial transformation used to generate the correspondences. From Table 1, our proposal was able to recover the correct transformation successfully. As it does filter the correspondences listed in the form of eliminating outliers, the needed total number of RANSAC iterations reduces drastically over all tested outlier ratios. Its success ratio is higher than running a RANSAC over all correspondences for the higher outlier ratios especially for 90%. Again from Table 1 and outlier ratio of 90%, increasing the total number of correspondences improved the performance of using our proposal (the column *with*) while the total number of successful trials for the column *without* remained approximately in the same level. This leads to the fact that the total number of inliers are more important than their ratio in our approach.

Algorithm 1: Experimental Simulations

Input: Image, I ; Transformations ($H_i, i = 1, 2, \dots, 20$), Outlier Ratios, o ; total number of correspondences, n ; $nbrRndTrials$

Extract features from image I

foreach H_i **do**

 Compute feature locations using H_i

foreach n in total number of correspondences **do**

 Select a subset of n correspondences as distributed as possible along image

foreach Outlier Ratio **do**

$t = 0$

repeat

 Generate outliers randomly by mismatching inliers

 Run the proposed method to get the geometrical invariant(s)

 Compute the transformation using filtered correspondences

 Check the correctness of obtained transformation

$t = t + 1$

until $t > nbrRndTrials$;

end

end

end

We repeated the same Algorithm 1 with a different step of generating outliers (see Algorithm 2). For this experiment, we added zero mean normally distributed additive noise with three different levels of σ , respectively 2.5, 5 and 10 to the certain number of feature point positions in one image to generate outliers. The results of this experiment are presented in Tables 2–4. The first three columns are for the total number of correspondences used, noise (σ) values and the transformation while the rest of the columns represent the number of random trials in which running RANSAC *with* our proposal and *without* were able to obtain the correct value of the transformation and average number of random iterations in RANSAC for each tested outlier ratio level. As the proposed method is mainly based on finding a peak in histogram, the total number of inliers is more important and it has a direct effect on the results. In RANSAC-based methods, both the outlier ratio and the total number of correspondences are important as the probability of selecting at least one outlier-free sample is a direct outcome of these values. This probability can be calculated as follows:

$$p = \prod_{i=0}^{s-1} \frac{n_{in} - i}{n - i}, \quad \sum p \approx (1 - (1 - p)^k), \quad (8)$$

where n_{in} is the total number of inliers, n is the total number of correspondences, s is the sample size (two or three; two is a minimum number of points to compute similarity transformation while three is for affine transformation.), p is the probability of selecting outlier free sample from the correspondences and k is the total number of random trials in RANSAC-based methods. Setting the value of k big enough, one could argue that RANSAC-based methods would choose at least one outlier-free sample. However, the bigger the k , the bigger the computational cost and this might not be suitable in real-time applications with low-computational resources available on board. From the experimental results, our approach overall was able to filter the correspondences and reduce the total number of outliers before applying robust estimation methods. From Table 2, in the presence of 90% of outliers and noise $\sigma = 2.5$, the total number of successful trials with the proposed approach is smaller than ones with the higher noise values for the most of the tested transformations (both $\sigma = 5$ and $\sigma = 10$) while the number of successful trials without using our proposal decreases with the high noise values (see Figure 4). For the three tested transformations, in the presence of low-level noise ($\sigma = 2.5$), using our approach did not provide better results compared to running RANSAC directly. This is mainly

due to the fact that the obtained values of geometrical invariants are prone to be sensitive and this makes it difficult to distinguish the real value. In the cases with higher noise, the correct geometrical values were spotted easily through histograms. In such a situation, we observed that increasing the precision would help.

Algorithm 2: Experimental Simulations

Input: Image, I ; Transformations ($H_i, i = 1, 2, \dots, 20$), Outlier Ratios, o ; Noise level, σ ; n number of correspondences; $nbrRndTrials$

Extract features from image I

foreach H_i **do**

 Compute feature locations using H_i

foreach n in total number of correspondences **do**

 Select a subset of n correspondences as distributed as possible along image

foreach σ in Noise level **do**

foreach o in Outlier Ratio **do**

$t = 0$

repeat

 Generate $n \times o$ outliers by adding normally distributed zero mean noise with σ standard deviation to randomly selected $n \times o$ correspondences.

 Run the proposed method to get the geometrical invariant(s)

 Compute the transformation using filtered correspondences

 Check the correctness of obtained transformation

$t = t + 1$

until $t > nbrRndTrials$;

end

end

end

end

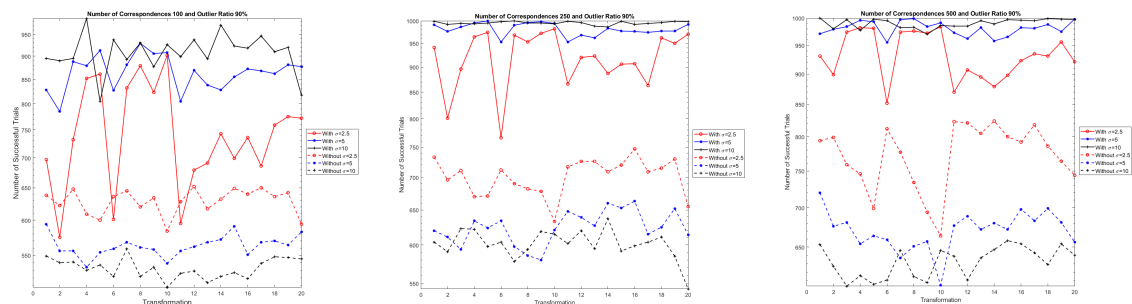


Figure 4. Total number of successful trials for each tested transformation for outlier ratio 90%. Increasing the noise level increased the performance of the proposed method for most of the tested transformations while it reduced running RANSAC *without* the proposed method.

Table 1. Experimental results from simulations outlined in Algorithm 1.

Number of Corresp.	Transformation	Outlier Ratio															
		75%				80%				85%				90%			
		Number of Successful Trials		Average Number of Iterations in RANSAC		Number of Successful Trials		Average Number of Iterations in RANSAC		Number of Successful Trials		Average Number of Iterations in RANSAC		Number of Successful Trials		Average Number of Iterations in RANSAC	
		without	with	without	with	without	with	without	with	without	with	without	with	without	with	without	with
100	1	1000	1000	438.87	1.09	999	1000	860.18	4.19	939	1000	1000	22.09	631	964	1000	152.89
	2	1000	1000	438.72	1.73	1000	1000	860.13	6.74	932	1000	1000	26.96	659	954	1000	176.96
	3	1000	1000	438.60	1.48	1000	1000	859.56	6.27	943	1000	1000	26.73	647	960	1000	156.50
	4	1000	1000	438.96	1.34	999	1000	860.68	5.54	943	1000	1000	24.92	629	966	1000	169.10
	5	1000	1000	438.77	1.52	998	1000	860.82	6.19	927	1000	1000	26.07	631	957	1000	182.35
	6	1000	1000	438.64	1.69	999	1000	860.67	6.97	938	1000	1000	26.95	649	949	1000	173.58
	7	1000	1000	438.83	1.55	998	1000	860.57	6.36	946	1000	1000	27.62	630	963	1000	165.56
	8	1000	1000	438.61	1.41	997	1000	860.49	5.91	936	1000	1000	26.04	615	958	1000	178.13
	9	1000	1000	438.88	2.02	999	1000	859.84	7.56	931	1000	1000	28.32	639	951	1000	180.55
	10	1000	1000	438.90	1.49	999	1000	860.00	6.45	951	1000	1000	26.00	650	961	1000	167.25
	11	1000	1000	438.71	1.63	999	1000	860.78	6.63	929	1000	1000	25.82	632	962	1000	163.30
	12	1000	1000	438.89	1.48	999	1000	860.33	6.33	941	1000	1000	25.43	638	966	1000	162.66
	13	1000	1000	438.85	1.87	997	1000	859.65	7.59	962	1000	1000	28.39	644	936	1000	178.02
	14	1000	1000	438.90	1.91	999	1000	860.88	7.49	943	1000	1000	28.16	643	955	1000	171.39
	15	1000	1000	438.86	1.76	999	1000	860.50	7.11	943	1000	1000	27.54	635	955	1000	175.68
	16	1000	1000	439.22	1.56	998	1000	860.77	6.51	940	1000	1000	26.79	609	963	1000	173.69
	17	1000	1000	438.84	1.41	1000	1000	860.29	6.07	932	1000	1000	25.42	635	969	1000	160.51
	18	1000	1000	438.81	1.51	1000	1000	860.08	6.12	930	1000	1000	26.26	647	957	1000	172.25
	19	1000	1000	438.83	1.73	1000	1000	860.53	7.10	943	1000	1000	27.62	645	963	1000	165.88
	20	1000	1000	439.06	2.78	998	1000	860.72	9.28	937	999	1000	32.41	632	945	1000	184.38
250	1	1000	1000	429.09	1.00	999	1000	859.87	1.00	968	1000	1000	1.03	654	1000	1000	8.54
	2	1000	1000	428.86	1.01	1000	1000	860.10	1.03	971	1000	1000	1.22	642	1000	1000	16.78
	3	1000	1000	428.86	1.00	1000	1000	860.33	1.01	972	1000	1000	1.16	629	1000	1000	15.93
	4	1000	1000	428.81	1.00	1000	1000	860.46	1.00	955	1000	1000	1.10	632	1000	1000	13.14
	5	1000	1000	428.90	1.00	999	1000	860.50	1.01	958	1000	1000	1.19	633	1000	1000	17.27
	6	1000	1000	428.88	1.03	998	1000	860.83	1.02	965	1000	1000	1.22	632	1000	1000	19.33
	7	1000	1000	428.96	1.01	1000	1000	860.25	1.02	962	1000	1000	1.15	624	999	1000	17.91
	8	1000	1000	428.74	1.00	1000	1000	860.10	1.02	952	1000	1000	1.13	643	1000	1000	13.64
	9	1000	1000	428.85	1.01	999	1000	860.45	1.05	964	1000	1000	1.42	622	1000	1000	21.92
	10	1000	1000	428.79	1.01	999	1000	860.34	1.02	958	1000	1000	1.17	611	1000	1000	18.21
	11	1000	1000	428.69	1.01	1000	1000	860.13	1.02	949	1000	1000	1.23	665	1000	1000	15.70
	12	1000	1000	428.62	1.00	1000	1000	860.15	1.01	972	1000	1000	1.12	610	1000	1000	14.29
	13	1000	1000	428.82	1.00	1000	1000	860.45	1.05	960	1000	1000	1.82	632	1000	1000	28.41
	14	1000	1000	428.67	1.01	1000	1000	859.85	1.02	971	1000	1000	1.65	647	999	1000	25.02
	15	1000	1000	428.76	1.01	1000	1000	860.30	1.03	950	1000	1000	1.44	636	1000	1000	23.54
	16	1000	1000	428.80	1.00	1000	1000	860.25	1.02	964	1000	1000	1.18	640	1000	1000	14.33
	17	1000	1000	428.78	1.00	1000	1000	860.10	1.02	961	1000	1000	1.15	632	1000	1000	13.39
	18	1000	1000	428.81	1.00	999	1000	860.19	1.02	970	1000	1000	1.14	634	1000	1000	13.53
	19	1000	1000	428.70	1.00	1000	1000	860.01	1.03	971	1000	1000	1.36	660	999	1000	22.09
	20	1000	1000	428.81	1.02	1000	1000	860.35	1.10	953	1000	1000	3.13	653	999	1000	32.08

Table 1. Cont.

Number of Corresp.	Transformation	Outlier Ratio															
		75%				80%				85%				90%			
		Number of Successful Trials		Average Number of Iterations in RANSAC		Number of Successful Trials		Average Number of Iterations in RANSAC		Number of Successful Trials		Average Number of Iterations in RANSAC		Number of Successful Trials		Average Number of Iterations in RANSAC	
		without	with	without	with	without	with	without	with	without	with	without	with	without	with	without	with
500	1	1000	1000	438.68	2.79	999	1000	860.26	3.34	950	1000	1000	5.96	643	1000	1000	30.36
	2	1000	1000	438.83	2.85	999	1000	860.23	3.53	965	1000	1000	8.95	657	1000	1000	35.72
	3	1000	1000	438.70	2.76	1000	1000	860.09	3.52	963	1000	1000	8.44	652	1000	1000	35.79
	4	1000	1000	439.00	2.82	1000	1000	860.15	3.32	962	1000	1000	7.21	614	999	1000	34.25
	5	1000	1000	438.88	2.87	1000	1000	860.09	3.44	961	1000	1000	8.23	635	1000	1000	38.62
	6	1000	1000	438.90	2.84	999	1000	860.53	3.50	958	1000	1000	8.70	629	1000	1000	38.56
	7	1000	1000	438.73	2.82	1000	1000	860.12	3.59	969	1000	1000	8.57	631	1000	1000	37.47
	8	1000	1000	438.89	2.81	1000	1000	860.09	3.43	962	1000	1000	8.10	667	1000	1000	34.73
	9	1000	1000	438.75	2.81	1000	1000	860.04	3.65	957	1000	1000	9.53	634	1000	1000	39.19
	10	1000	1000	439.13	2.76	1000	1000	860.41	3.51	965	1000	1000	8.72	629	1000	1000	36.94
	11	1000	1000	438.68	2.80	1000	1000	860.04	3.46	960	1000	1000	8.54	630	1000	1000	36.04
	12	1000	1000	438.79	2.75	1000	1000	860.50	3.47	961	1000	1000	7.94	620	1000	1000	35.04
	13	1000	1000	438.60	2.81	1000	1000	860.26	3.61	953	1000	1000	9.62	641	1000	1000	39.41
	14	1000	1000	438.81	2.83	1000	1000	860.22	3.60	949	1000	1000	9.86	647	1000	1000	39.41
	15	1000	1000	438.73	2.78	1000	1000	860.28	3.56	955	1000	1000	9.26	626	1000	1000	37.94
	16	1000	1000	438.62	2.81	1000	1000	860.25	3.43	963	1000	1000	8.04	635	1000	1000	34.24
	17	1000	1000	438.73	2.83	999	1000	860.49	3.46	968	1000	1000	7.47	654	1000	1000	33.28
	18	1000	1000	438.72	2.74	999	1000	860.44	3.50	964	1000	1000	7.36	636	1000	1000	34.14
	19	1000	1000	438.79	2.80	999	1000	859.89	3.58	959	1000	1000	9.03	633	1000	1000	37.85
	20	1000	1000	438.77	2.85	999	1000	860.34	4.11	965	1000	1000	12.90	634	1000	1000	41.79

Table 2. Experimental results from simulations through adding different levels of noise to correspondences with a total number of 100 correspondences.

Number of Corresp.	Noise σ	Transformation	Outlier Ratio															
			75%		80%		85%		90%									
			Number of Successful Trials	Average Number of Iterations in RANSAC	Number of Successful Trials	Average Number of Iterations in RANSAC	Number of Successful Trials	Average Number of Iterations in RANSAC	Number of Successful Trials	Average Number of Iterations in RANSAC								
			without	with	without	with	without	with	without	with								
100	2.5	1	1000	1000	422.38	17.12	1000	998	822.24	22.25	973	979	1000	66.44	638	697	1000	247.77
		2	1000	1000	427.47	26.68	998	1000	824.89	45.24	966	990	1000	75.14	622	575	1000	403.28
		3	1000	1000	430.38	15.48	1000	1000	839.92	31.65	952	997	1000	54.92	648	732	1000	331.70
		4	1000	1000	432.22	13.46	1000	1000	844.44	24.24	961	998	1000	50.04	609	852	1000	262.85
		5	1000	1000	434.62	14.17	999	1000	847.44	23.59	963	998	1000	51.14	600	861	1000	281.51
		6	1000	998	424.53	26.90	1000	990	825.58	48.63	957	953	1000	134.35	636	601	1000	365.58
		7	1000	1000	430.12	15.80	1000	999	835.41	34.53	960	995	1000	65.38	645	832	1000	245.39
		8	1000	1000	433.27	17.51	1000	1000	845.14	21.94	953	1000	1000	49.53	620	879	1000	269.25
		9	1000	1000	434.17	16.24	1000	1000	848.40	26.46	965	1000	1000	44.74	634	823	1000	318.33
		10	1000	1000	436.62	11.60	999	1000	854.00	22.50	961	1000	1000	36.90	584	902	1000	286.92
		11	1000	1000	422.47	26.58	999	992	815.03	40.11	969	953	1000	103.61	628	595	999	353.94
		12	1000	1000	422.35	20.47	1000	994	813.67	47.30	966	964	1000	98.23	652	679	1000	283.07
		13	1000	999	423.85	25.81	999	1000	824.05	43.80	964	979	1000	109.86	617	691	1000	368.18
		14	1000	1000	425.23	21.80	999	998	824.60	40.44	969	970	1000	117.16	632	743	1000	328.18
		15	1000	1000	424.09	28.28	1000	997	826.24	50.82	967	966	1000	111.34	649	699	1000	364.10
		16	1000	1000	423.53	23.23	999	995	825.22	38.66	960	963	1000	94.46	640	736	999	280.46
		17	1000	999	425.46	21.62	1000	996	828.31	31.28	966	984	1000	82.94	650	686	1000	294.11
		18	1000	999	426.26	18.53	1000	1000	831.02	31.60	978	979	1000	83.28	636	759	1000	299.63
		19	1000	1000	429.59	20.74	999	1000	835.25	35.59	970	990	1000	71.29	642	775	1000	336.23
		20	1000	1000	432.04	20.80	1000	1000	843.39	31.85	964	996	1000	82.86	594	772	1000	438.50
100	5	1	1000	1000	434.59	9.24	999	999	850.68	19.81	945	1000	1000	40.58	594	828	999	286.74
		2	1000	1000	435.73	16.67	999	1000	852.04	26.87	949	1000	1000	60.01	556	785	999	342.96
		3	1000	1000	436.75	12.13	1000	1000	854.93	20.63	940	1000	1000	52.16	556	888	1000	272.93
		4	1000	1000	437.33	11.00	1000	1000	857.50	17.41	957	1000	1000	38.96	534	879	1000	303.93
		5	1000	1000	438.09	9.94	1000	1000	858.35	18.96	956	1000	1000	40.14	554	913	1000	288.07
		6	1000	999	435.23	14.62	1000	999	853.42	28.07	949	995	1000	68.56	559	827	1000	304.31
		7	1000	1000	436.66	12.62	1000	1000	853.73	22.03	951	998	1000	48.92	568	881	1000	285.86
		8	1000	1000	437.73	11.49	1000	1000	857.93	18.35	936	1000	1000	38.41	561	929	1000	233.94
		9	1000	1000	437.83	12.62	998	1000	858.48	21.28	949	999	1000	42.14	558	906	1000	281.63
		10	1000	1000	438.31	9.17	1000	1000	859.51	18.78	947	1000	1000	37.64	539	908	1000	262.63
		11	1000	1000	434.53	15.93	1000	1000	850.21	27.40	942	997	1000	58.08	556	805	1000	315.21
		12	1000	1000	434.91	14.62	997	999	851.59	27.66	960	991	1000	61.29	562	869	1000	270.01
		13	1000	1000	435.16	17.53	999	1000	851.54	31.34	946	999	1000	63.62	568	838	1000	358.61
		14	1000	1000	435.37	17.86	999	1000	852.95	25.48	939	1000	1000	58.41	572	828	1000	356.95
		15	1000	1000	434.58	19.03	999	1000	850.59	29.86	949	995	1000	72.93	591	855	1000	325.13
		16	1000	1000	435.41	16.71	998	1000	851.03	24.07	955	996	1000	56.25	551	872	1000	258.49
		17	1000	1000	435.76	15.41	1000	1000	853.31	25.86	954	1000	1000	54.36	568	868	1000	259.37
		18	1000	1000	436.06	13.21	1000	1000	854.21	21.20	950	998	1000	59.14	570	862	1000	297.56
		19	1000	1000	437.17	13.34	1000	1000	853.18	23.59	950	1000	1000	44.79	564	881	1000	306.86
		20	1000	1000	437.97	15.31	1000	1000	856.75	28.14	942	1000	1000	51.78	583	877	1000	390.24

Table 2. Cont.

Number of Corresp.	Noise σ	Transformation	Outlier Ratio															
			75%				80%				85%				90%			
			Number of Successful Trials		Average Number of Iterations in RANSAC		Number of Successful Trials		Average Number of Iterations in RANSAC		Number of Successful Trials		Average Number of Iterations in RANSAC		Number of Successful Trials		Average Number of Iterations in RANSAC	
			without	with	without	with												
100	10	1	1000	1000	438.25	8.76	999	1000	858.73	19.29	940	1000	1000	35.93	549	895	1000	277.67
		2	1000	1000	438.65	12.09	1000	1000	859.00	22.09	949	1000	1000	37.03	540	890	1000	299.06
		3	1000	1000	438.41	9.75	1000	1000	859.70	17.45	937	1000	1000	40.06	541	895	999	325.11
		4	1000	1000	438.39	8.03	1000	1000	860.09	15.71	949	1000	1000	36.14	530	988	1000	101.85
		5	1000	1000	438.52	6.90	1000	1000	860.27	14.94	937	1000	1000	37.63	537	805	1000	423.70
		6	1000	1000	438.37	12.89	999	1000	859.49	22.05	956	1000	1000	36.71	522	937	1000	198.73
		7	1000	1000	439.22	9.08	999	1000	859.61	19.64	935	1000	1000	36.97	559	893	1000	308.48
		8	1000	1000	438.85	6.67	1000	1000	859.79	17.87	943	1000	1000	36.00	522	930	1000	255.70
		9	1000	1000	438.66	9.24	1000	1000	860.50	20.30	948	1000	1000	37.63	534	877	1000	328.77
		10	1000	1000	439.06	6.91	1000	1000	860.35	15.48	943	1000	1000	34.40	508	926	1000	249.76
		11	1000	1000	438.12	11.08	998	1000	859.15	21.56	950	1000	1000	46.94	526	899	1000	283.15
		12	1000	1000	437.84	13.51	1000	1000	856.90	19.14	949	1000	1000	39.72	529	937	1000	240.97
		13	1000	1000	438.60	11.10	999	1000	858.78	20.63	947	1000	1000	42.65	514	894	999	314.33
		14	1000	1000	438.12	12.28	998	1000	859.39	21.90	939	1000	1000	40.07	522	972	1000	179.03
		15	1000	1000	438.06	11.84	1000	1000	857.70	21.95	935	1000	1000	39.19	527	923	1000	271.82
		16	1000	1000	438.12	11.18	999	1000	858.92	22.29	951	1000	1000	38.02	519	918	1000	277.09
		17	1000	1000	438.31	12.03	1000	1000	859.14	20.45	942	1000	1000	40.12	539	946	1000	225.12
		18	1000	1000	438.00	10.32	999	1000	858.27	19.62	943	1000	1000	39.50	548	910	1000	277.68
		19	1000	1000	438.82	10.24	999	1000	859.80	21.59	954	1000	1000	36.81	547	920	1000	280.26
		20	1000	1000	438.71	10.74	1000	1000	860.16	19.79	933	1000	1000	39.29	545	817	1000	449.70

Table 3. Experimental results from simulations through adding different levels of noise to correspondences with a total number of 250 correspondences.

Number of Corresp.	Noise σ	Transformation	Outlier Ratio															
			75%				80%				85%				90%			
			Number of Successful Trials		Average Number of Iterations in RANSAC		Number of Successful Trials		Average Number of Iterations in RANSAC		Number of Successful Trials		Average Number of Iterations in RANSAC		Number of Successful Trials		Average Number of Iterations in RANSAC	
			without	with	without	with	without	with	without	with	without	with	without	with	without	with		
250	2.5	1	1000	1000	433.28	7.73	1000	1000	819.85	12.78	983	994	1000	32.14	733	941	1000	86.58
		2	1000	997	435.94	32.31	1000	998	824.42	37.53	978	982	1000	69.99	696	801	1000	267.96
		3	1000	1000	440.31	10.15	999	1000	837.23	15.05	970	998	1000	29.51	711	896	1000	154.72
		4	1000	1000	442.37	8.22	999	1000	844.88	12.33	978	1000	1000	24.63	670	964	1000	113.48
		5	1000	1000	444.53	6.40	998	1000	847.38	11.59	968	1000	1000	18.90	671	974	1000	112.26
		6	1000	1000	433.31	36.66	999	998	822.78	59.31	969	956	1000	125.89	712	766	1000	305.23
		7	1000	1000	440.80	9.28	1000	1000	836.15	15.18	979	998	1000	28.18	690	968	1000	101.58
		8	1000	1000	443.20	8.26	1000	1000	844.56	12.82	963	1000	1000	23.14	682	953	1000	130.63
		9	1000	1000	444.99	10.60	1000	1000	848.88	15.65	970	999	1000	31.74	678	972	1000	115.78
		10	1000	1000	446.77	5.47	1000	1000	853.80	8.71	957	1000	1000	20.62	633	982	1000	109.07
		11	1000	1000	432.11	13.37	1000	998	816.18	20.74	985	992	1000	52.45	717	866	1000	152.35
		12	1000	1000	432.17	11.18	1000	1000	816.97	19.86	985	991	1000	37.95	726	920	1000	111.43
		13	1000	1000	432.93	11.03	1000	1000	818.91	24.94	984	992	1000	55.25	726	923	1000	171.26
		14	1000	1000	434.90	18.87	1000	998	821.12	20.56	983	991	1000	47.00	709	887	1000	185.86
		15	1000	1000	435.20	13.29	1000	1000	821.99	27.17	992	993	1000	47.11	720	906	1000	179.29
		16	1000	1000	433.88	11.84	1000	1000	819.17	17.55	979	992	1000	43.37	747	907	1000	137.29
		17	1000	999	435.12	11.64	1000	1000	825.55	18.50	984	995	1000	43.38	709	863	1000	161.55
		18	1000	1000	437.65	10.33	1000	999	829.66	15.99	975	994	1000	31.88	715	962	1000	103.18
		19	1000	1000	440.25	11.88	1000	999	834.00	15.45	981	1000	1000	34.77	730	950	1000	124.94
		20	1000	1000	442.36	10.05	1000	1000	840.73	20.81	977	999	1000	36.88	655	970	1000	145.78
250	5	1	1000	1000	446.02	5.62	1000	1000	850.43	8.983	962	998	1000	15.56	620	991	1000	66.05
		2	1000	1000	446.76	8.88	1000	1000	853.51	16.215	969	1000	1000	25.50	611	976	1000	119.56
		3	1000	1000	447.96	5.79	1000	1000	855.34	9.192	960	1000	1000	19.73	594	986	1000	77.27
		4	1000	1000	448.23	4.52	1000	1000	856.72	6.996	952	1000	1000	15.21	634	995	1000	81.61
		5	1000	1000	448.78	4.15	1000	1000	857.39	6.413	968	1000	1000	14.64	624	1000	1000	55.80
		6	1000	1000	445.89	14.11	1000	1000	851.11	19.352	967	1000	1000	35.50	634	953	1000	161.34
		7	1000	1000	447.80	5.64	999	1000	854.32	9.014	952	1000	1000	16.34	598	990	1000	74.82
		8	1000	1000	448.36	4.48	1000	1000	857.26	7.388	968	1000	1000	13.89	586	996	1000	54.56
		9	1000	1000	448.78	5.72	1000	1000	858.02	10.126	949	1000	1000	15.22	580	998	1000	65.13
		10	1000	1000	449.21	2.60	1000	1000	858.85	5.584	954	1000	1000	12.99	621	994	1000	72.94
		11	1000	1000	445.52	10.20	1000	1000	848.65	12.948	967	998	1000	24.80	648	953	1000	129.81
		12	1000	1000	445.22	7.81	1000	1000	848.99	13.473	971	999	1000	26.42	639	968	1000	111.93
		13	1000	1000	446.30	10.47	1000	1000	850.77	17.686	974	999	1000	35.46	627	962	1000	164.56
		14	1000	1000	446.30	8.96	999	1000	850.11	14.528	959	999	1000	29.74	660	983	1000	122.98
		15	1000	1000	446.04	7.99	1000	1000	852.35	15.486	977	998	1000	28.23	653	977	1000	116.60
		16	1000	1000	445.77	8.10	999	1000	850.49	13.961	962	1000	1000	27.57	663	976	1000	105.22
		17	1000	1000	445.95	7.75	999	1000	853.24	11.681	958	1000	1000	20.57	615	974	1000	93.35
		18	1000	1000	446.97	7.37	1000	1000	852.21	11.06	963	1000	1000	20.70	625	977	1000	113.94
		19	1000	1000	447.65	7.08	1000	1000	854.52	12.457	960	1000	1000	21.00	652	977	1000	113.21
		20	1000	1000	448.11	8.35	999	1000	857.03	12.463	951	1000	1000	25.87	614	992	1000	100.31

Table 3. Cont.

Number of Corresp.	Noise σ	Transformation	Outlier Ratio															
			75%				80%				85%				90%			
			Number of Successful Trials		Average Number of Iterations in RANSAC		Number of Successful Trials		Average Number of Iterations in RANSAC		Number of Successful Trials		Average Number of Iterations in RANSAC		Number of Successful Trials		Average Number of Iterations in RANSAC	
			without	with	without	with	without	with	without	with	without	with	without	with	without	with	without	with
250	10	1	1000	1000	449.12	3.11	999	1000	858.17	5.36	960	1000	1000	12.62	604	999	1000	50.60
		2	1000	1000	449.08	5.05	999	1000	858.84	8.75	965	1000	1000	16.60	591	992	1000	75.63
		3	1000	1000	449.52	2.96	998	1000	859.58	5.58	955	1000	1000	13.35	623	994	1000	58.33
		4	1000	1000	449.74	2.08	998	1000	860.16	3.86	956	1000	1000	9.17	622	993	1000	93.89
		5	1000	1000	449.65	1.77	1000	1000	859.80	3.67	958	1000	1000	10.32	598	995	1000	90.75
		6	1000	1000	449.58	5.86	999	1000	858.52	9.79	955	1000	1000	21.17	604	998	1000	57.01
		7	1000	1000	449.37	3.04	1000	1000	859.70	5.53	959	1000	1000	12.81	578	1000	1000	41.49
		8	1000	1000	449.56	1.94	1000	1000	859.85	3.85	954	1000	1000	9.46	594	995	1000	78.09
		9	1000	1000	449.66	2.41	999	1000	860.26	4.78	942	1000	1000	11.86	619	995	1000	53.26
		10	1000	1000	450.09	1.31	1000	1000	860.60	2.42	962	1000	1000	8.14	615	993	1000	92.71
		11	1000	1000	449.14	5.84	1000	1000	858.21	9.68	965	1000	1000	15.63	602	999	1000	50.76
		12	1000	1000	449.17	5.57	1000	1000	857.86	9.08	955	1000	1000	16.88	620	996	1000	68.86
		13	1000	1000	449.04	5.90	1000	1000	858.30	11.06	959	1000	1000	19.49	595	988	1000	117.74
		14	1000	1000	449.26	6.13	1000	1000	858.49	10.95	954	1000	1000	18.51	637	986	1000	123.33
		15	1000	1000	448.80	5.37	998	1000	858.77	9.77	957	1000	1000	21.27	592	999	1000	54.57
		16	1000	1000	449.27	4.10	1000	1000	858.49	8.17	960	1000	1000	15.94	599	992	1000	80.88
		17	1000	1000	449.08	4.02	1000	1000	858.20	7.50	956	1000	1000	15.94	604	994	1000	77.48
		18	1000	1000	449.31	4.04	1000	1000	858.70	7.69	959	1000	1000	15.51	611	996	1000	71.31
		19	1000	1000	449.56	3.96	998	1000	859.78	6.54	957	1000	1000	15.68	585	999	1000	62.72
		20	1000	1000	449.54	4.07	999	1000	859.79	7.55	945	1000	1000	16.71	543	998	1000	44.11

Table 4. Experimental Results from simulations through adding different levels of noise to correspondences with a total number of 500 correspondences.

Number of Corresp.	Noise σ	Transformation	Outlier Ratio															
			75%				80%				85%				90%			
			Number of Successful Trials		Average Number of Iterations in RANSAC		Number of Successful Trials		Average Number of Iterations in RANSAC		Number of Successful Trials		Average Number of Iterations in RANSAC		Number of Successful Trials		Average Number of Iterations in RANSAC	
			without	with	without	with												
500	2.5	1	1000	999	423.79	11.58	1000	1000	816.46	15.84	994	996	1000	30.47	794	931	1000	119.65
		2	1000	1000	425.48	18.04	1000	1000	824.93	28.88	995	992	1000	59.54	799	899	1000	202.91
		3	1000	1000	430.17	11.75	1000	1000	836.86	23.05	991	999	1000	28.79	759	974	1000	112.30
		4	1000	1000	432.21	10.94	999	1000	843.61	14.80	984	1000	1000	28.14	746	982	1000	101.92
		5	1000	1000	433.70	8.66	1000	1000	846.70	17.75	978	999	1000	29.09	699	981	1000	87.64
		6	1000	999	423.46	25.10	1000	998	821.96	39.43	996	990	1000	66.67	812	852	1000	222.88
		7	1000	1000	430.42	12.41	1000	1000	837.60	17.33	990	999	1000	29.88	777	974	1000	124.03
		8	1000	1000	433.19	11.36	1000	1000	843.51	15.25	986	1000	1000	30.49	734	976	1000	107.25
		9	1000	1000	434.39	12.84	1000	1000	848.51	18.13	985	1000	1000	32.57	694	972	1000	125.78
		10	1000	1000	436.36	7.01	1000	1000	853.78	12.93	976	1000	1000	18.81	664	984	1000	114.13
		11	1000	999	421.46	14.13	1000	999	815.82	26.83	992	994	1000	45.39	823	870	1000	157.58
		12	1000	1000	421.61	11.82	1000	997	815.72	20.49	998	991	1000	49.12	821	907	1000	141.68
		13	1000	999	423.54	18.67	1000	993	822.36	30.44	996	981	1000	64.86	805	895	1000	151.15
		14	1000	1000	424.02	17.39	1000	1000	819.90	30.34	990	989	1000	59.79	824	879	1000	182.19
		15	1000	1000	424.60	15.58	1000	999	821.47	27.16	993	994	1000	46.53	800	898	1000	187.97
		16	1000	1000	423.42	14.89	1000	996	818.55	24.88	994	991	1000	43.72	792	923	1000	143.92
		17	1000	1000	425.17	11.68	1000	999	823.24	23.64	985	996	1000	42.86	818	935	1000	130.19
		18	1000	1000	426.42	14.04	1000	1000	828.49	20.46	994	998	1000	33.29	786	931	1000	129.03
		19	1000	1000	429.28	14.14	1000	1000	832.88	21.06	991	999	1000	37.41	764	956	1000	135.25
		20	1000	1000	431.89	15.06	1000	999	842.12	21.52	983	998	1000	38.55	744	921	1000	233.27
500	5	1	1000	1000	434.93	7.78	1000	1000	850.33	13.99	981	1000	1000	24.37	720	971	1000	120.87
		2	1000	1000	435.99	10.93	1000	1000	851.88	19.45	967	1000	1000	27.31	676	979	1000	97.61
		3	1000	1000	436.62	7.51	1000	1000	855.04	13.35	970	1000	1000	23.28	681	984	1000	111.50
		4	1000	1000	437.56	6.12	1000	1000	856.59	12.46	981	1000	1000	20.62	654	996	1000	64.90
		5	1000	1000	438.16	7.45	1000	1000	858.04	12.50	976	1000	1000	19.43	664	993	1000	68.05
		6	1000	1000	435.18	14.57	1000	1000	851.13	21.66	971	1000	1000	34.07	659	955	1000	168.24
		7	1000	1000	436.98	6.26	1000	1000	854.50	12.43	972	1000	1000	24.27	637	997	1000	71.15
		8	1000	1000	437.50	6.84	999	1000	856.76	11.53	981	1000	1000	20.59	651	999	1000	54.86
		9	1000	1000	437.78	9.97	1000	1000	857.82	13.45	968	1000	1000	24.37	657	984	1000	99.33
		10	1000	1000	438.34	6.37	999	1000	859.31	11.54	974	1000	1000	19.00	605	991	1000	82.95
		11	1000	1000	434.32	9.57	1000	1000	849.61	18.56	985	999	1000	36.72	677	973	1000	126.36
		12	1000	1000	434.77	12.02	1000	1000	848.47	16.56	977	1000	1000	36.06	689	962	1000	141.92
		13	1000	1000	435.45	15.03	1000	1000	850.44	22.30	983	1000	1000	39.98	672	982	1000	132.29
		14	1000	1000	435.30	11.21	1000	1000	851.38	18.60	976	1000	1000	36.10	680	958	1000	164.39
		15	1000	1000	434.89	10.89	1000	1000	850.91	18.55	983	1000	1000	34.46	672	965	1000	151.29
		16	1000	1000	435.21	11.15	1000	1000	850.69	21.00	987	999	1000	32.54	698	982	1000	105.75
		17	1000	1000	435.37	11.08	1000	1000	851.89	17.74	985	1000	1000	24.61	683	981	1000	112.17
		18	1000	1000	436.00	10.20	1000	1000	852.62	12.60	981	1000	1000	28.83	699	988	1000	84.40
		19	1000	1000	437.05	9.17	1000	1000	854.41	17.55	979	1000	1000	29.13	681	975	1000	142.21
		20	1000	1000	437.28	12.54	1000	1000	856.12	14.87	976	1000	1000	32.35	656	998	1000	69.47

Table 4. Cont.

Number of Corresp.	Noise σ	Transformation	Outlier Ratio															
			75%				80%				85%				90%			
			Number of Successful Trials		Average Number of Iterations in RANSAC		Number of Successful Trials		Average Number of Iterations in RANSAC		Number of Successful Trials		Average Number of Iterations in RANSAC		Number of Successful Trials		Average Number of Iterations in RANSAC	
			without	with	without	with	without	with	without	with	without	with	without	with	without	with	without	with
500	10	1	1000	1000	438.04	5.67	1000	1000	858.27	12.42	975	1000	1000	17.65	653	1000	1000	56.22
		2	1000	1000	438.09	7.25	999	1000	859.15	11.79	968	1000	1000	23.78	627	980	1000	136.20
		3	1000	1000	438.45	5.08	1000	1000	859.17	9.55	959	1000	1000	19.30	604	997	1000	58.39
		4	1000	1000	438.62	3.30	1000	1000	860.10	8.90	961	1000	1000	17.42	616	977	1000	116.75
		5	1000	1000	438.89	4.90	1000	1000	860.12	8.91	965	1000	1000	18.03	606	998	1000	47.00
		6	1000	1000	437.97	7.77	1000	1000	858.30	14.24	971	1000	1000	20.05	611	995	1000	74.06
		7	1000	1000	438.75	6.31	1000	1000	859.36	11.08	958	1000	1000	17.98	646	982	1000	104.44
		8	1000	1000	438.62	4.69	998	1000	860.49	7.34	973	1000	1000	18.66	615	983	1000	102.88
		9	1000	1000	438.64	5.73	1000	1000	860.13	9.39	969	1000	1000	19.50	608	970	1000	121.62
		10	1000	1000	438.92	3.77	1000	1000	860.39	4.56	960	1000	1000	14.94	646	986	1000	79.16
		11	1000	1000	437.94	6.58	1000	1000	857.99	13.74	969	1000	1000	24.45	639	985	1000	121.74
		12	1000	1000	437.79	8.21	1000	1000	858.15	12.89	976	1000	1000	29.12	611	985	1000	106.40
		13	1000	1000	438.33	8.46	1000	1000	858.16	14.34	958	1000	1000	22.82	637	995	1000	96.97
		14	1000	1000	438.02	6.15	1000	1000	858.23	11.75	977	1000	1000	22.35	647	989	1000	104.91
		15	1000	1000	438.10	7.88	1000	1000	858.51	14.89	967	1000	1000	23.00	658	997	1000	87.27
		16	1000	1000	437.88	7.72	999	1000	858.28	11.93	967	1000	1000	20.67	654	996	1000	68.42
		17	1000	1000	438.24	7.74	1000	1000	858.55	10.11	968	1000	1000	19.67	643	995	1000	67.35
		18	1000	1000	438.41	5.58	1000	1000	858.96	12.08	966	1000	1000	21.02	629	999	1000	54.84
		19	1000	1000	438.47	5.78	999	1000	859.52	11.18	976	1000	1000	22.41	654	998	1000	56.64
		20	1000	1000	438.65	7.39	1000	1000	859.62	11.69	976	1000	1000	26.25	640	997	1000	50.63

Although our implementation is not optimized, its computational burden is still low and it is within the time saved in RANSAC iterations. Its time saving can be coarsely estimated by comparing the iteration numbers needed in RANSAC. If the confidence value is low, we also form additional triangles using bucketing [17]. Feature points are grouped into a 10×10 cells distributed uniformly. One feature from each cell randomly picked and used as a corner for forming triangles. The total number of triangles can be a maximum of $\binom{100}{3}$ assuming that each cell has at least one feature point and selected features are not collinear. The best would be to use all the possible triangles; however, this would bring a prohibitively huge computational burden. The total number of triangles used can be adjusted depending on the computational resources available. We also observed that increasing the size of the selected correspondences (m) in the sorted list as a resulting step of geometrical invariant computation can improve the result; however, this would also increase the total number of iterations needed in RANSAC.

4.2. Experiment 2

In this experiment, we tested the proposed approach on challenging real images from seabed captured using an underwater robot while surveying a coral reef patch [13]. Some samples are given in Figure 5. SIFT [14] is employed to extract and match features. Afterward, we ran our proposal to use geometrical invariants to filter out outliers. We run RANSAC algorithm 1000 times over initially matched features (referred to as *without* in Table 5) and remaining matched features after applying our proposal (referred to as *with* in Table 5). During the experiment, the maximum number of iterations for RANSAC was limited to also 1000 (max. $k = 1000$ in Equation (8)). The total number of RANSAC iterations and the total number of inliers computed using the resulting motion of RANSAC steps are given in Table 5. The threshold in RANSAC to decide whether an inlier was selected or not as 2.5 pixels and errors in one image were minimized to estimate the motion [3]. For the image pairs in gray-rows, the confidence level was greater than the selected threshold; therefore, our algorithm was able to skip the robust estimation part and the total number of inliers were 89, 268, and 275, respectively. For comparison purposes, we also opted to provide the results of applying RANSAC in the table for those image pairs. An average number of RANSAC iterations are given in Figure 6.

As it was mentioned before, increasing the total number of inliers would improve the performance of our proposal. In order to test this claim using real data, we resized images for the pairs in which we had less than 200 correspondences (image pairs numbered 2, 17, 19, 21, 23, and 24 in Table 5) with a scaling factor of 1.5 with the expectation of increasing the total number of detected correspondences and inliers. We run our proposal on the newly detected correspondences. Obtained results are presented in Table 6. From the table, it can be observed that the total number of inliers was increased and this could be expected as the total number of correspondences, and thus inliers, increased. However, this would not always be guaranteed as it can be noticed with the image pair 24. Our approach failed to recover stable geometrical invariants due to the low number of inliers. In pairs (2, 17, 19, and 23), the average number of RANSAC iterations reduced compared to the ones in Table 5. This is a result of the expected increment in the total number of inliers along with the total number of correspondences. One could argue that applying a more aggressive threshold in descriptor matching could improve the inlier ratio. This would be also favorable for our approach as it would be likely to skip the robust estimation step due to the higher value of confidence.

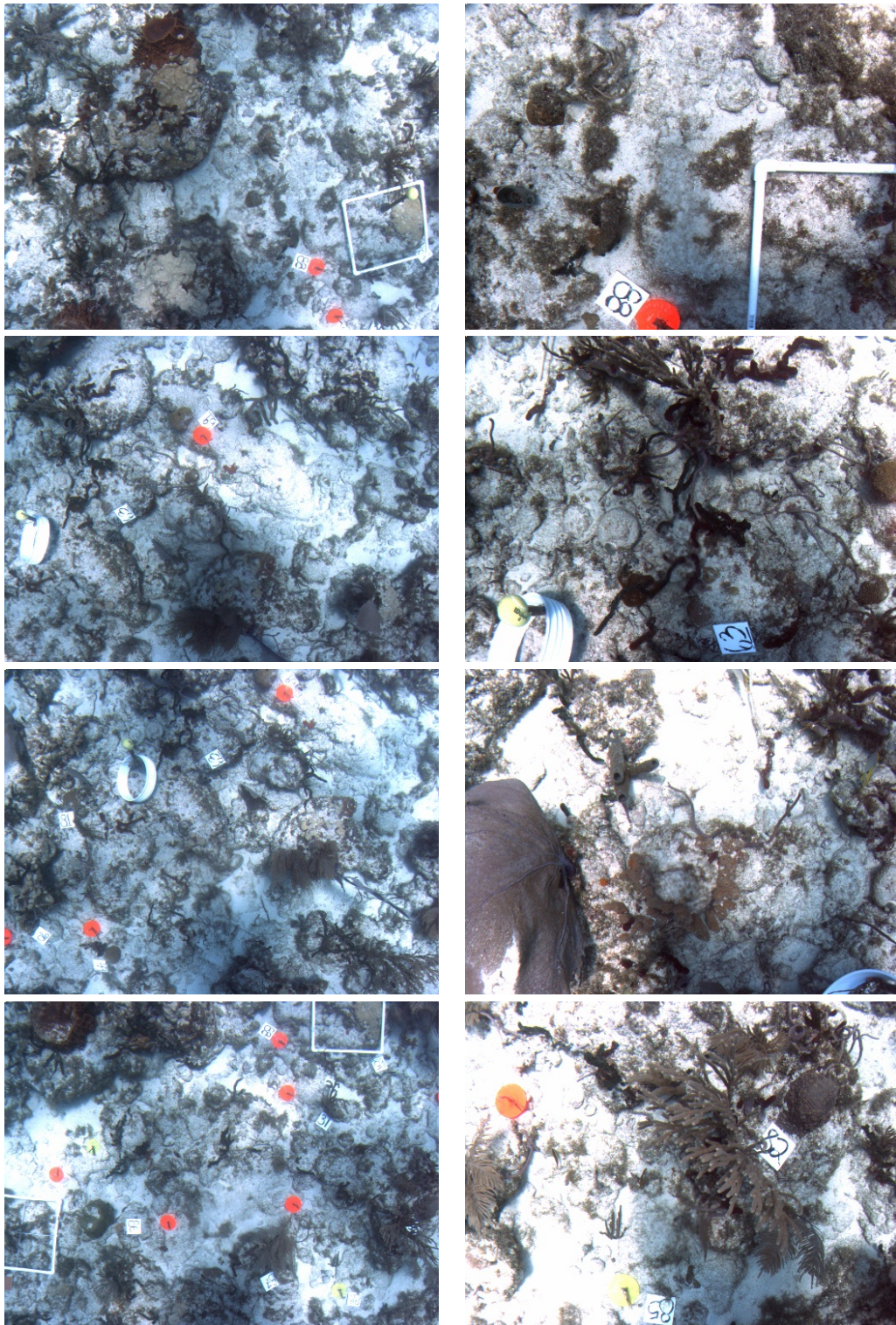


Figure 5. Rows show some sample image pairs used in the experiments. They are corresponding to Image Pairs 1, 3, 19 and 24 in Table 5. The resolution of images is 512×384 .

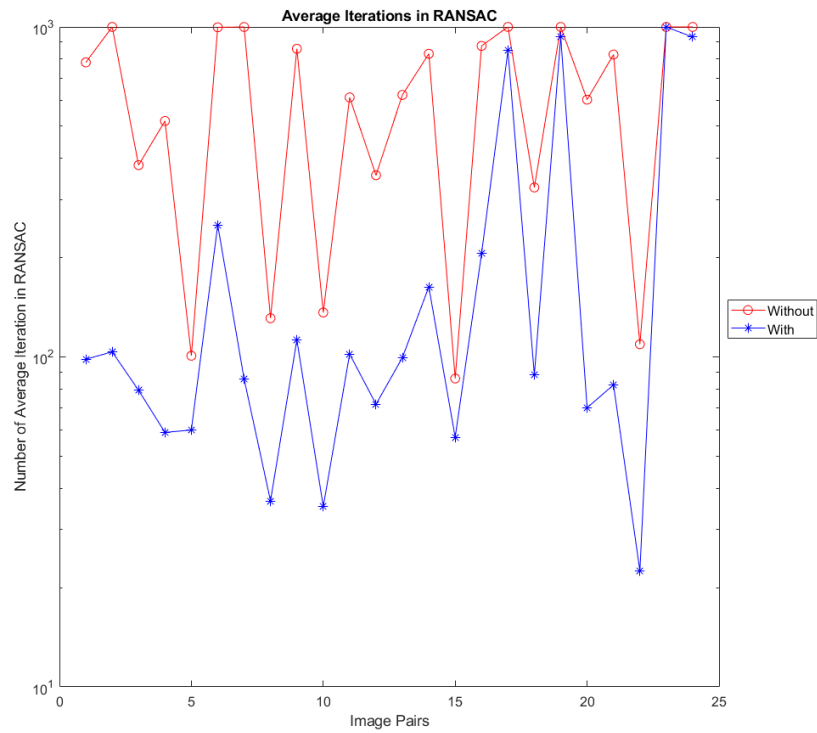


Figure 6. Average number of iterations in RANSAC with the proposed approach and without. For four of the image pairs, our proposal has similar performance on average, while, for the remaining pairs, it reduced the iteration number needed in RANSAC.

Table 5. Experimental results obtained using real data of underwater images.

Image Pair	Number of Corresp.	Number of Iterations in RANSAC								Number of Inliers							
		without				with				without				with			
		Min.	Max.	Avg.	Std.	Min.	Max.	Avg.	Std.	Min.	Max.	Avg.	Std.	Min.	Max.	Avg.	Std.
1	236	514	1000	780.74	105.39	60	156	98.36	16.3	59	91	81.65	3.65	60	91	80.81	3.44
2	148	1000	1000	1000.00	0.00	89	208	103.60	15.3	6	19	16.78	2.92	17	19	18.33	0.70
3	354	234	635	381.24	63.43	52	124	79.21	12.8	109	148	134.34	4.68	80	146	131.45	6.98
4	526	356	732	518.77	68.83	40	94	59.04	9.08	110	140	130.93	5.35	77	124	107.60	7.22
5	680	68	152	100.81	14.14	41	87	60.05	8.25	255	315	300.17	9.9	258	314	300.06	9.08
6	252	881	1000	997.41	14.44	176	391	251.09	32	37	52	46.82	2.95	21	38	26.56	2.37
7	223	961	1000	999.84	2.46	50	166	85.69	17.8	32	50	48.66	2.82	45	51	49.32	0.60
8	375	84	230	131.02	24.90	24	70	36.61	7.78	171	194	184.26	2.7	167	191	184.84	1.62
9	268	583	1000	858.85	119.29	68	183	112.66	17.9	30	49	45.78	4.18	24	49	34.85	4.44
10	306	83	243	136.33	26.13	18	65	35.20	7.62	155	164	159.09	1.99	156	163	159.78	0.80
11	249	385	903	611.46	85.97	71	158	101.98	15	55	84	77.00	2.54	70	82	76.28	2.46
12	293	261	554	355.28	49.98	48	114	71.88	11.4	94	111	102.77	2.45	69	105	95.56	5.21
13	304	406	942	622.35	80.30	57	152	99.56	16.6	39	65	54.69	3.91	39	66	56.15	4.38
14	360	582	1000	829.27	92.79	114	223	163.05	21.7	79	106	92.63	3.77	80	106	91.42	3.27
15	839	53	128	86.03	13.04	36	91	57.06	9.34	327	417	390.33	15.3	320	416	390.99	15.47
16	266	570	1000	876.05	102.93	162	367	205.72	35.5	54	77	66.06	3.07	22	61	43.79	9.97
17	166	1000	1000	1000.00	0.00	699	1000	847.74	97.9	18	31	25.24	2.9	14	24	21.89	1.73
18	406	198	554	326.17	57.14	47	151	88.10	15.7	139	179	167.56	6.96	127	180	166.12	7.99
19	138	1000	1000	1000.00	0.00	680	1000	933.63	125	5	16	13.10	2.09	5	16	13.30	1.95
20	200	414	913	601.97	71.21	44	111	70.13	9.96	55	67	58.14	2.76	55	66	58.16	2.00
21	196	531	1000	824.81	118.15	46	130	82.28	14.9	26	40	36.37	2.72	19	36	29.98	2.08
22	290	69	194	109.24	18.91	13	44	22.47	4.35	90	116	109.81	4.34	95	116	109.37	4.17
23	171	1000	1000	1000.00	0.00	1000	1000	1000.00	0	13	32	24.75	3.43	13	31	25.70	4.08
24	148	1000	1000	1000.00	0.00	737	1000	931.62	112	4	16	11.80	2.12	10	14	11.39	1.56

Table 6. Experimental results obtained with increasing image size.

Image Pair	Number of Corresp.	Number of Iterations in RANSAC								Number of Inliers							
		without				with				without				with			
		Min.	Max.	Avg.	Std.	Min.	Max.	Avg.	Std.	Min.	Max.	Avg.	Std.	Min.	Max.	Avg.	Std.
2	533	1000	1000	1000	0	21	57	29.00	4.88	47	93	88.62	3.31	84	91	88.807	1.04
17	545	1000	1000	1000	0	59	214	122.04	22.70	5	60	38.23	10.53	35	57	49.284	4.94
19	406	1000	1000	1000	0	459	1000	680.11	135.27	4	23	10.37	5.25	14	24	21.879	0.65
21	500	1000	1000	1000	0	86	292	160.86	36.00	30	57	50.80	6.43	24	35	31.176	2.23
23	457	1000	1000	1000	0	356	916	650.29	94.78	8	49	36.64	7.34	21	48	42.496	3.62
24	439	1000	1000	1000	0	1000	1000	1000.00	0.00	4	25	15.24	5.46	0	4	2.336	1.97

5. Conclusions

Camera carrying Unmanned Underwater Vehicles have been widely used for different purposes such as inspection, mapping, sample collection, and many others. When these vehicles do not have a wide variety of sensors, image (or video) data are the only source of information and image matching (or registration) is one of most fundamental steps of optical mapping, navigation and localization. Since distinctive point extraction and matching steps provide a set of correspondences that do not obey the common motion of the camera, image registration pipeline employs robust estimation methods to remove such correspondences. In this paper, we present a method for identifying geometrical invariants to filter the outliers before the robust estimation step, aiming to reduce the time they needed and to improve their performance. We also discussed that their usage can be omitted in some cases. We provide experimental results with both synthetic and real data to show the efficiency and limitations of the proposed method.

Author Contributions: Conceptualization, A.E. and N.Y.C.; software and validation, A.E.; writing—original draft preparation, A.E.; writing—review and editing, N.Y.C.

Funding: This research received no external funding and the APC was funded by JAIST Faculty research budget.

Acknowledgments: The authors would like to thank Nuno Gracias from the Computer Vision and Robotics Group of University of Girona for providing the dataset used in experiments. Figure 2 is used from [3] with the permission of Cambridge University Press through PLSclear Ref. No:14046. obtained on 10 May 2019.

Conflicts of Interest: The authors declare no conflict of interest.

Abbreviations

The following abbreviations are used in this manuscript:

DOF	Degree of Freedom
RANSAC	Random Sampling Consensus
MSAC	M-estimator Sample Consensus
MLESAC	Maximum Likelihood Estimator Sample Consensus
PROSAC	Progressive Sample Consensus
SIFT	Scale Invariant Feature Transform

Appendix A. List of Transformations Used in Experiments

For experiments, we used 20 different affine transformation [15]. For some of the projective model transformations, we set (3, 1) and (3, 2) elements of their matrices to 0 manually. Following the decomposition in Equation (2), we list the parameter vector $[\lambda_1, \lambda_2, \theta, \phi]$ for the transformations used in experiments in Table A1. Warped images of a sample image using the these transformations are given in Table A2.

Table A1. Transformation parameters used in experiments.

Transformation	λ_1	λ_2	θ (In Rad.)	ϕ (In Rad.)
1	0.89	0.88	-0.24	0.97
2	0.74	0.73	-0.69	-2.51
3	0.54	0.53	-1.39	-2.45
4	0.43	0.42	0.15	-3.06
5	0.39	0.33	-0.71	-2.88
6	0.82	0.82	-0.55	-2.36
7	0.57	0.52	2.62	-0.25
8	0.41	0.40	-2.09	-0.61
9	0.33	0.33	-0.40	1.85
10	0.26	0.23	2.68	0.10
11	1.01	0.87	-0.27	1.13
12	1.07	0.82	0.34	1.33
13	1.22	0.61	-0.47	1.28
14	1.20	0.60	0.09	1.29
15	1.23	0.60	0.66	1.43
16	0.92	0.79	-0.02	1.63
17	0.90	0.67	-0.04	1.66
18	0.88	0.55	-0.05	1.67
19	0.87	0.41	-0.09	1.68
20	0.91	0.26	-0.11	1.68

Table A2. Warped images with transformations used in Experiment 1. The numbers below each image represent the transformation parameters listed in Table A1.

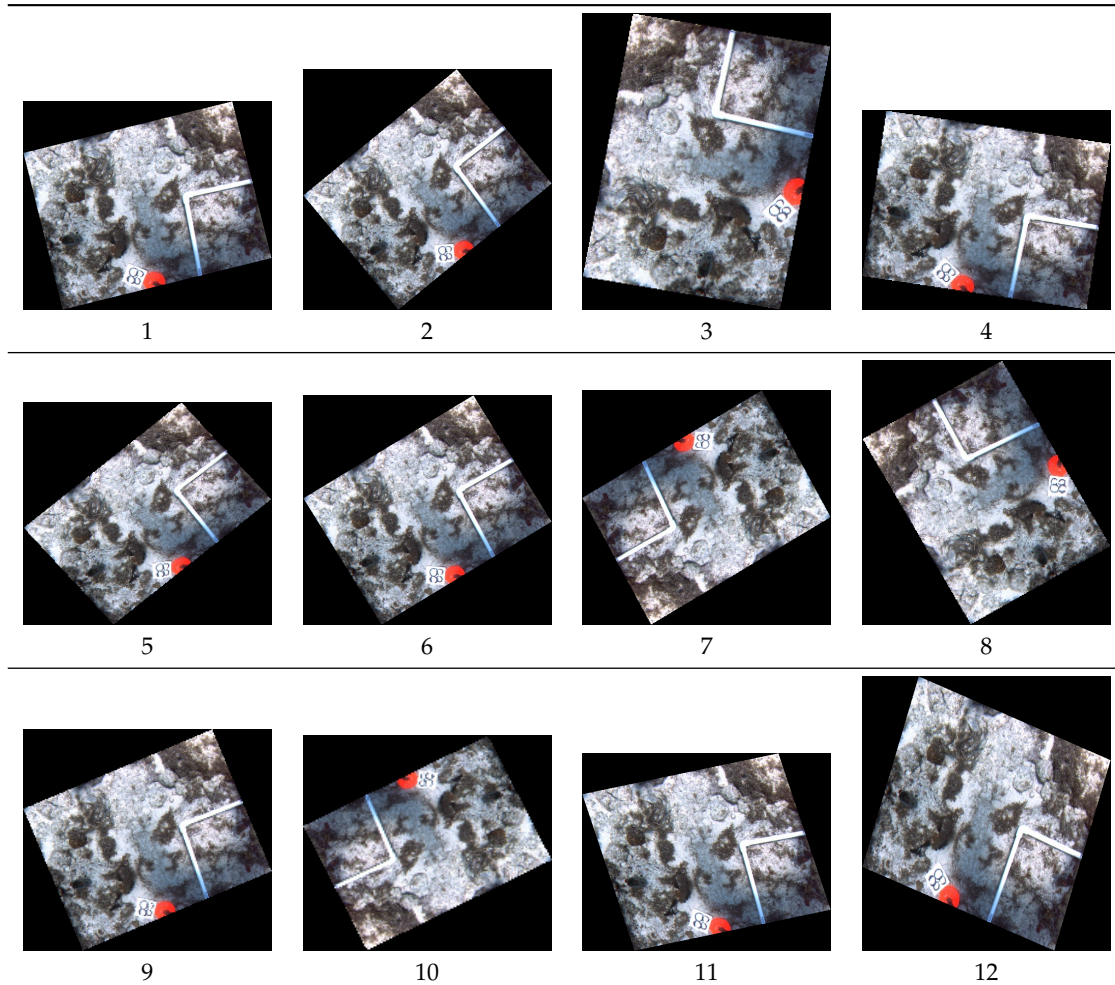
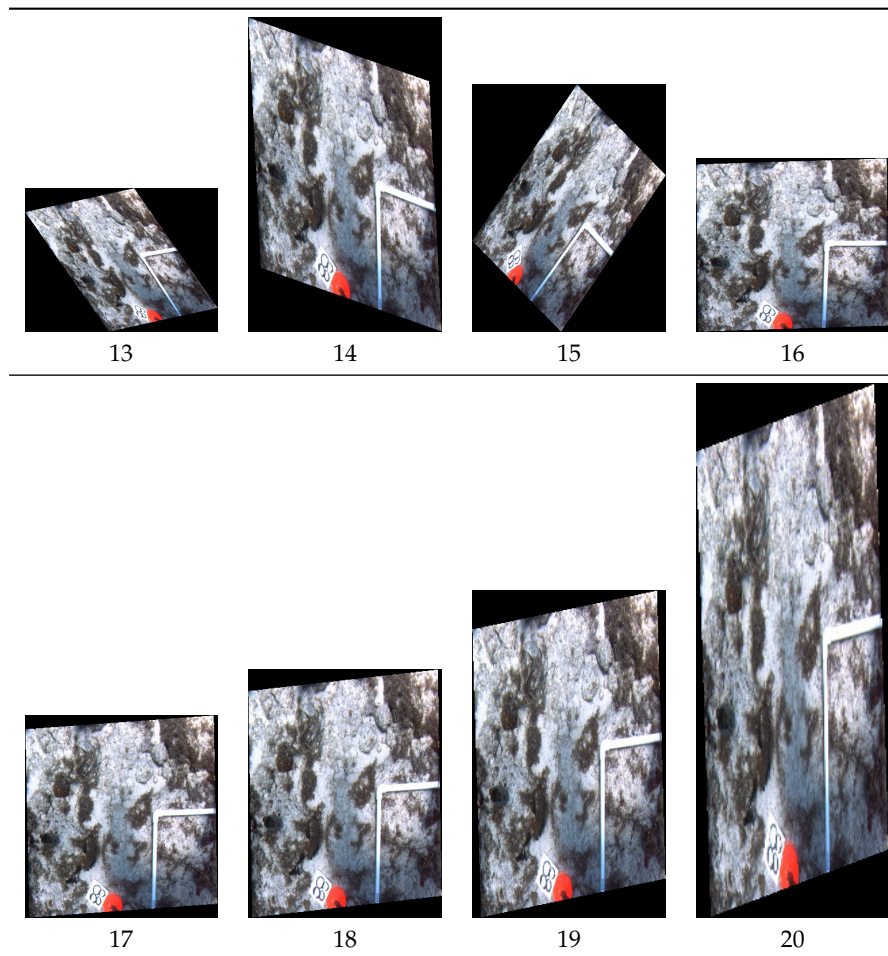


Table A2. Cont.



References

1. Zitová, B.; Flusser, J. Image registration methods: A survey. *Image Vis. Comput.* **2003**, *21*, 977–1000. [[CrossRef](#)]
2. Fischler, M.A.; Bolles, R.C. Random sample consensus: A paradigm for model fitting with applications to image analysis and automated cartography. *Commun. ACM* **1981**, *24*, 381–395. [[CrossRef](#)]
3. Hartley, R.; Zisserman, A. *Multiple View Geometry in Computer Vision*, 2nd ed.; Cambridge University Press: Cambridge, UK, 2004.
4. Torr, P.; Zisserman, A. MLESAC: A New Robust Estimator with Application to Estimating Image Geometry. *Comput. Vis. Image Underst.* **2000**, *78*, 138–156. [[CrossRef](#)]
5. Tordoff, B.J.; Murray, D.W. Guided-MLESAC: Faster Image Transform Estimation by Using Matching Priors. *IEEE Trans. Pattern Anal. Mach. Intell.* **2005**, *27*, 1523–1535. [[CrossRef](#)] [[PubMed](#)]
6. Chum, O.; Matas, J. Matching with PROSAC. *Proc. Comput. Vis. Pattern Recognit.* **2005**, *1*, 220–226.
7. Raguram, R.; Frahm, J.-M.; Pollefeys, M. A Comparative Analysis of RANSAC Techniques Leading to Adaptive Real-Time Random Sample Consensus. In *Computer Vision—ECCV 2008*; Lecture Notes in Computer Science; Springer: Berlin/Heidelberg, Germany, 2008; Volume 5303, pp. 500–513.
8. Senthilnath, J.; Kalro, N.P.; Benediktsson, J.A. Accurate point matching based on multi-objective Genetic Algorithm for multi-sensor satellite imagery. *Appl. Math. Comput.* **2014**, *236*, 546–564. [[CrossRef](#)]
9. Le, V.-H.; Vu, H.; Nguyen, T.T.; Le, T.-L.; Tran, T.-H. Acquiring qualified samples for RANSAC using geometrical constraints. *Pattern Recognit. Lett.* **2018**, *102*, 58–66.
10. Marszalek, M.; Rokita, P. Pattern matching with differential voting and median transformation derivation improved point-pattern matching algorithm for two-dimensional coordinate lists. *Comput. Imaging Vis.* **2006**, *32*, 1002–1007.

11. Reiss, T.H. *Recognizing Planar Objects Using Invariant Image Features*; Lecture Notes in Computer Science; Springer: Berlin/Heidelberg, Germany, 1993; Volume 676.
12. Byer, O.; Lazebnik, F.; Smeltzer, D.L. *Methods for Euclidean Geometry*; Mathematical Association of America: Washington, DC, USA, 2010.
13. Gracias, N.; Negahdaripour, S. Underwater mosaic creation using video sequences from different altitudes. In Proceedings of the OCEANS 2005 MTS/IEEE, Washington, DC, USA, 17–23 September 2005; Volume 2, pp. 1295–1300.
14. Lowe, D.G. Distinctive image features from scale-invariant keypoints. *Int. J. Comput. Vis.* **2004**, *60*, 91–110. [[CrossRef](#)]
15. Datasets from Visual Geometry Group, Department of Engineering Science, University of Oxford. Available online: <http://www.robots.ox.ac.uk/~vgg/data/data-aff.html> (accessed on 30 November 2018).
16. Kovesi, P.D. MATLAB and Octave Functions for Computer Vision and Image Processing. Available online: <http://www.peterkovesi.com/matlabfns/> (accessed on 30 November 2018).
17. Choukroun, A.; Charvillat, V. *Bucketing Techniques in Robust Regression for Computer Vision*; Lecture Notes in Computer Science; Springer: Berlin/Heidelberg, Germany, 2003; Volume 2749, pp. 609–616.



© 2019 by the authors. Licensee MDPI, Basel, Switzerland. This article is an open access article distributed under the terms and conditions of the Creative Commons Attribution (CC BY) license (<http://creativecommons.org/licenses/by/4.0/>).